



Paleoenvironments of a proglacial lake in Schirmacher Oasis, East Antarctica: Insights from quartz grain microtextures

Abhijit MAZUMDER^{1*}, Pawan GOVIL¹, Ratan KAR¹,
Narath Meethal GAYATHRI² and RAGHURAM³

¹ Birbal Sahni Institute of Palaeosciences,
53 University Road, Lucknow – 226 007, India

² Department of Marine Geology and Geophysics, School of Marine Sciences,
Cochin University of Science and Technology, Cochin – 16, India

³ Polar Studies Division, Geological Survey of India,
Faridabad, Haryana – 121 001, India

* Corresponding author: <abhijit_mazumder@bsip.res.in> <abhimazumder@gmail.com>

Abstract: Eighteen sediment samples from a 36 cm long sediment core retrieved from a proglacial lake (namely P 11) situated in the Schirmacher Oasis, East Antarctica, were analysed for the study of quartz grain morphology and microtexture, along with sand percentage, to reconstruct the paleoenvironmental changes in the lake during the Holocene. The age of the core ranges from 3.3 ka BP to 13.9 ka BP. The quartz grain morphology and microtexture reveal significant evidences of glacial transport along with some eolian and aqueous activities. On the basis of predominance of these signatures and the zonation from CONISS Cluster Analysis on the percentages of characteristic grain morphology and microtextures, the entire core has been subdivided into three major zones. From the paleoenvironmental perspective, it can be concluded that there is an onset of interglacial period at the advent of Holocene (12.3 ka BP), which reigned until 5.3 ka BP and thereafter, again a glacial environment prevailed until 3.3 ka BP with some variations in-between. The results indicate probable alternative colder and less colder phases in the study area, which are also well supported by the respective sand percentages in the sediments.

Key words: Antarctica, Dronning Maud Land Proglacial lake, Holocene, Quartz grains, microtexture, sand percentage, CONISS Cluster Analysis.

Introduction

The Schirmacher Oasis (70°44'21"–70°46'04"S to 11°26'03"–11°49'54"E), a 25 km long and 3 km wide ice-free plateau along the Princess Astrid Coast in Dronning Maud Land, East Antarctica, consists of more than 100 freshwater lakes, including epishelf, land-locked and proglacial lakes. The oasis is situated on an average 100 m above the sea level between the Antarctic Ice Sheet and the Novolazarevskaya Ice Shelf. This region has significance for paleoclimatic and paleoenvironmental studies, as it is one of larger coastal oases in East Antarctica. To decipher the past climatic changes, the lacustrine sediments of this region should be addressed as they preserve the geological history. However, Schirmacher Oasis has still remained a less worked region in Antarctica with reference to paleoclimatic studies of lake sediments (Bera 2004; Sharma *et al.* 2007; Phartiyal *et al.* 2011; Phartiyal 2014; Warriar *et al.* 2014, 2016; Mahesh *et al.* 2015).

Paleoenvironmental studies can be carried out with a use of variable proxies. Terrigenous autochthonous mineral grains reflect the signatures of the interaction between different geological processes, *e.g.* provenance of sediments, nature and grade of weathering processes and transportation (Last 2001). Hence, these grains can be used to decipher the past changes in basin shape and size (Olsen 1990; Henderson and Last 1998), and paleoclimatic oscillations within the catchment area (Menking 1997; Schütt 1998). In colder regions, quartz is one of the few important detrital minerals, which has been successfully used to reconstruct the past climatic changes, because of their response to physical weathering processes (Chamley 1989; Pistolato *et al.* 2006). Quartz grains have higher preservation potential due to their resistance to weathering compared to any other predominantly available minerals present in the lake sediments (Krinsley and Doornkamp 1973; Mahaney 1995, 2002). These grains can be derived from various provenances, such as, mechanically or chemically derived quartz grains, wind-driven aeolian quartz and biogenic silica consisting mostly of diatoms (Stanley and DeDecker 2002). Quartz grain microtextures and morphology, like grain shape, fracture patterns, step patterns *etc.*, depend primarily on the conditions of transportation and deposition, and hence provide records of the past environment and climate (Whalley and Krinsley 1974; Mahaney *et al.* 1996; Helland and Holmes 1997; Hart 2006; Mathur *et al.* 2009). The studies of such quartz grains under Scanning Electron Microscope (SEM) can reveal the details of different geological processes that the grains have undergone during transportation and deposition (Mahaney 1995; Strand *et al.* 2003). In the present study, a lacustrine sediment core was analysed to identify the paleoenvironmental history of a proglacial lake in Schirmacher Oasis during the Holocene with the help of quartz grain microtextures and morphology.

Methods

A 36 cm long sediment core was collected by sediment corer from a proglacial lake (namely P 11; Lat. $70^{\circ}45'58.83''\text{S}$, Long. $11^{\circ}42'45.19''\text{E}$; maximum depth of the lake 2 m; ~ 400 m from the Indian Antarctic Station *Maitri*) in the Schirmacher Oasis (Fig. 1). The core was subsampled at 2 cm intervals to obtain 18 samples for further study. Approximately 5 g of sediments from each interval were processed for quartz grain analysis following the sample preparation procedure described by Krinsley and Doornkamp (1973). Twenty quartz grains ($>63 \mu\text{m}$) from each sample (total 360 grains) were separated manually with the help of binocular



Fig. 1. Location of the coring site and proglacial lakes in Schirmacher Oasis, East Antarctica (A) and actual field photograph of the studied lake (B).

stereomicroscope to document the grain morphology and surface microtextures under SEM (model no. LEO 430). Grain morphology and surface microtextures have been studied and interpreted to understand the transport mechanism and depositional environment of the sediments following the method adopted from Krinsley and Doornkamp (1973), Mahaney (1995), Helland and Holmes (1997), Strand *et al.* (2003) and Vos *et al.* (2014). The percentage of different features of grain morphology and microtextures is also tabulated and used for Constrained Incremental Sum of Squares (CONISS) Cluster Analysis with the help of Tilia Software Program Version 1.7.16 (Grimm 2011) to understand the different environments of sedimentation. On the other hand, 5 g of sediments from each interval was processed following the methodology prescribed by Krumbein and Pettijohn (1938) to acquire sand sized particles ($>63 \mu\text{m}$), and the relative percentage of sand at each interval was calculated and tabulated to exhibit the down-core variation in sand percentage. The lithology of the core was also plotted against the sand percentage variation along the core.

AMS dates of the bulk sediment from three lithological intervals were obtained from the Radiocarbon Laboratory, Silesian University of Technology, Poland (funded by Birbal Sahni Institute of Palaeosciences, Lucknow, India); sample record index No. 2708; Job No. NB-29/RIF/2014.

Results

The quartz grains studied under SEM exhibit textures that originated from mechanical actions (Figs. 2 and 3). The majority of quartz grains show high to moderate angularity (Figs. 2.1–6, 9, 10, 12; Figs. 3.14, 15, 17, 21–24) with sub-rounded to rounded grains (Figs. 2.7, 11 and Figs. 3.18–20) and exhibit microtextures with moderate to high relief. Each grain shows characteristic microtextures of mechanical origin, such as edge rounding, large and small conchoidal fractures, arcuate steps, straight steps, large breakage blocks, freshly broken smooth surfaces, parallel to subparallel linear striations, oriented as well as random scratches and grooves, pitted surface or collision pits and featureless smooth surfaces (Figs. 2.1–6, 9–10, 12 and Figs. 3.14, 16, 17, 21–24). Some textures of chemical origin, *viz.* adhering particles, silica precipitation, etched surfaces and solution channels are also present (Figs. 2.8 and Fig. 3.13, 16, 19, 20, 22).

On the basis of these characters (Tables 1 and 2), the entire core can be subdivided into three major parts. The upper part until 10 cm shows high angularity (65–75%), high relief (55–65%), large conchoidal fractures (60–70%), arcuate steps (30–50%), large breakage blocks (35–65%), and freshly broken smooth surfaces (10–25%). The middle part (10–30 cm) shows high roundness

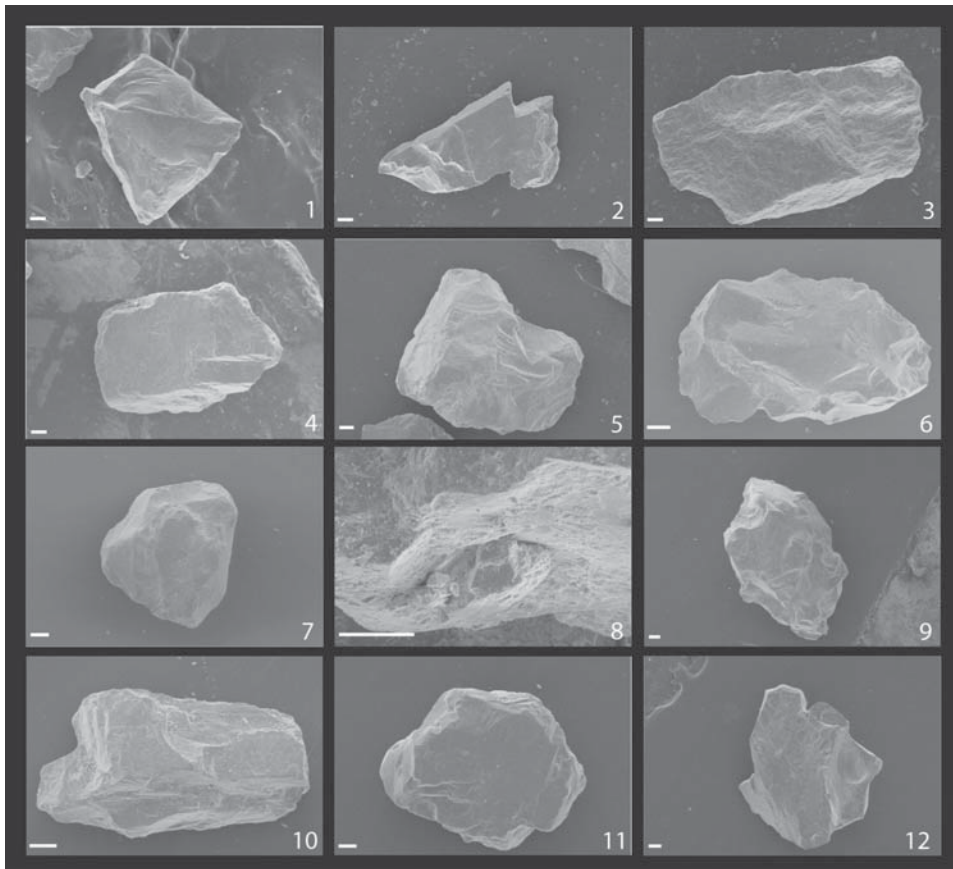


Fig. 2. Scanning Electron Micro-photographs of quartz grains for studying their morphology and microtextures (the sample intervals are given within parentheses, explanations of each microtextures are tabulated in Table 1): **1.** Angular grain with arcuate fracture pattern (0–2 cm); **2.** Angular grain with breakage block (0–2 cm); **3.** Sub-angular grain with oriented scratches and grooves (2–4 cm); **4.** Sub-angular grain with breakage blocks (4–6 cm); **5.** Angular grain with large conchoidal fractures (6–8 cm); **6.** Sub-angular grain with breakage block, arcuate fractural pattern and large conchoidal fractures (8–10 cm); **7.** Sub-rounded grain, with rounder edge (10–12 cm); **8.** Grain with silica precipitation and adhering particles (12–14 cm); **9.** Sub-angular grain with large conchoidal fractures (12–14 cm); **10.** Sub-angular grain with sub-parallel to parallel steps (14–16 cm); **11.** Sub-rounded grain (14–16 cm); **12.** Sub-angular grain with large conchoidal fractures (16–18 cm). All scale bars 100 mm.

(40–65%), low relief (50–70%), edge rounding (55–75%), small conchoidal fractures (20–40%), random grooves and scratches (30–50%), pitted surfaces and collision pits (20–40%), featureless smooth surfaces (5–40%), silica precipitation (5–25%), adhering particles (10–50%), etched surfaces (0–10%) and solution channels (0–10%). The lowest part (30–36 cm) shows high angularity (65–85%), high relief (60–75%), large conchoidal fractures (45–70%), arcuate steps

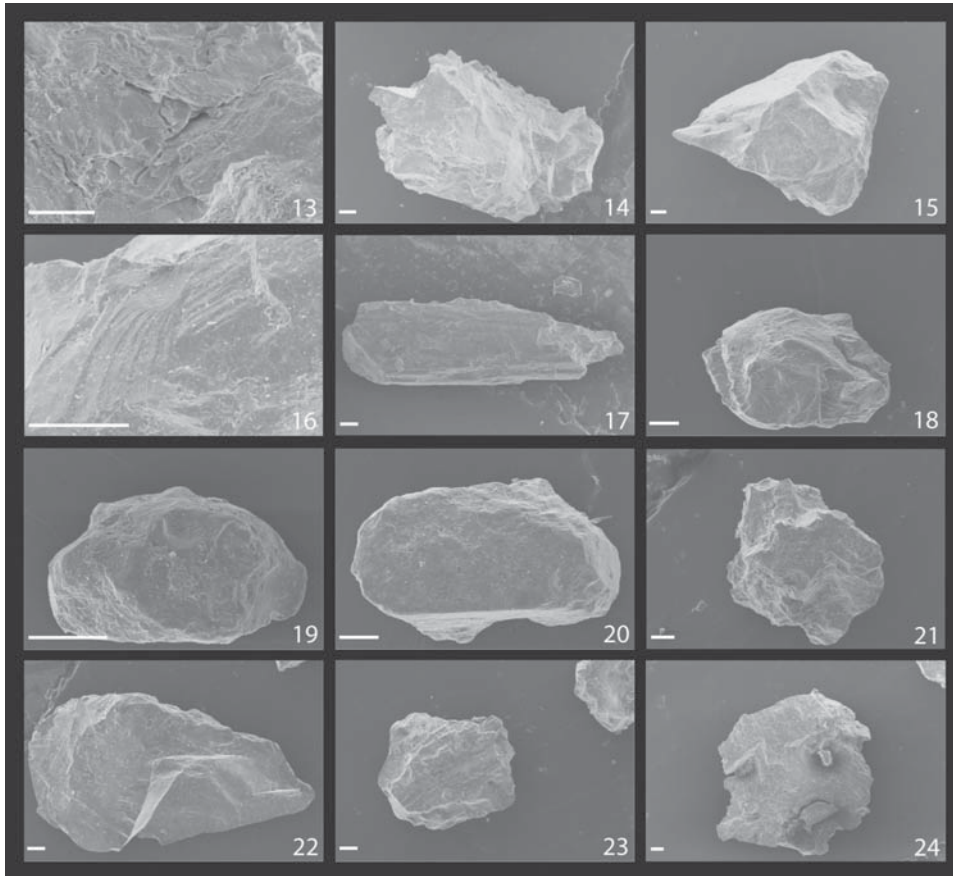


Fig. 3. Scanning Electron Micro-photographs of quartz grains for studying their morphology and microtextures (the sample intervals are given within parentheses, explanations of each microtextures are tabulated in Table 1): **13.** Grain with solution channels (16–18 cm); **14.** Angular grain with breakage blocks (18–20 cm); **15.** Angular grain (20–22 cm); **16.** Grain with parallel to sub-parallel steps and adhering particles (20–22 cm); **17.** Angular grain with parallel steps (22–24 cm); **18.** Sub-rounded grain (24–26 cm); **19.** Sub-rounded grain with silica precipitation and adhering particles (24–26 cm); **20.** Sub-rounded grain with adhering particles (26–28 cm); **21.** Sub-angular grain with random scratches and grooves (28–30 cm); **22.** Sub-angular grain with sub-parallel to parallel striations with adhering particles (30–32 cm); **23.** Sub-angular grain with oriented scratches and grooves (32–34 cm); **24.** Sub-angular grain with arcuate fracture pattern and parallel striations (34–36 cm). All scale bars 100 μ m.

(15–45%), large breakage blocks (30–40%), freshly broken surfaces (5–45%), subparallel linear striations (25–50%) and oriented grooves and scratches (30–45%); refer to Table 2.

The CONISS cluster analysis (Fig. 4) shows three prominent zones at 2.0 level of total sum of squares based on the percentages of different characteristics of grain morphology and microtextures. Zone I consists of five samples falling

Table 1

List of important quartz grain microtextures found in the core samples and their implications.

| Core Interval (cm) | Main Microtextures of Quartz Grain | Environmental Significance | Overall Environment | |
|--------------------|------------------------------------|---|--------------------------|---|
| 0–10 | 0–2 | Angular grains with arcuate fracture pattern and breakage blocks | Glacial | GLACIAL |
| | 2–4 | Sub-angular grains with oriented scratches and grooves | Glacial | |
| | 4–6 | Sub-angular grains with breakage blocks | Glacial | |
| | 6–8 | Angular grains with large conchoidal fractures | Glacial | |
| | 8–10 | Sub-angular grains with breakage blocks, arcuate and large conchoidal fractures | Glacial | |
| 10–30 | 10–12 | Sub-rounded grains with rounded edge | Eolian | GLACIAL WITH AQUEOUS AND EOLIAN INFLUENCE |
| | 12–14 | Silica precipitation, adhering particles, sub-angular and large conchoidal fracture | Glacial, Aqueous | |
| | 14–16 | Sub-rounded to sub-angular grains with sub-parallel to parallel steps | Glacial, Eolian | |
| | 16–18 | Sub-angular grains with large conchoidal fractures and solution channels | Glacial, Aqueous | |
| | 18–20 | Angular grains with breakage blocks | Glacial | |
| | 20–22 | Angular grains with parallel to sub-parallel steps and adhering particles | Glacial, Aqueous | |
| | 22–24 | Angular grains with parallel steps | Glacial | |
| | 24–26 | Sub-rounded grains with silica precipitation, and adhering particles | Glacial, Aqueous, Eolian | |
| | 26–28 | Sub-rounded grains with adhering particle | Glacial, Aqueous, Eolian | |
| | 28–30 | Sub-angular grains with random scratches and grooves | Glacial, Eolian | |
| 30–36 | 30–32 | Sub-angular grains with sub-parallel to parallel striations | Glacial | GLACIAL |
| | 32–34 | Sub-angular grains with oriented scratches and grooves | Glacial | |
| | 34–36 | Sub-angular grains with arcuate fracture pattern and parallel striations | Glacial | |

Table 2 continued

| Sample intervals | 20–22 cm | 22–24 cm | 24–26 cm | 26–28 cm | 28–30 cm | 30–32 cm | 32–34 cm | 34–36 cm |
|--------------------------------|----------|----------|----------|----------|----------|----------|----------|----------|
| <i>Morphological Textures</i> | | | | | | | | |
| Angularity | 40 | 45 | 35 | 40 | 50 | 65 | 75 | 85 |
| Roundness | 60 | 55 | 65 | 60 | 50 | 35 | 25 | 15 |
| High relief | 40 | 50 | 40 | 45 | 50 | 70 | 60 | 75 |
| Low relief | 60 | 50 | 60 | 55 | 50 | 30 | 40 | 25 |
| <i>Mechanical Textures</i> | | | | | | | | |
| Edge rounding | 60 | 55 | 60 | 60 | 55 | 40 | 40 | 15 |
| Large conchoidal fractures | 25 | 20 | 15 | 5 | 10 | 45 | 55 | 70 |
| Small conchoidal fractures | 25 | 30 | 35 | 30 | 25 | 15 | 20 | 25 |
| Arcuate steps | 15 | 5 | 10 | 5 | 10 | 15 | 20 | 45 |
| Straight steps | 10 | 15 | 5 | 10 | 10 | 20 | 40 | 45 |
| Large breakage blocks | 5 | 15 | 10 | 5 | 5 | 40 | 40 | 30 |
| Freshly broken smooth surfaces | | | | | | 5 | 30 | 45 |
| Subparallel linear striations | 10 | 5 | 10 | 15 | 10 | 45 | 25 | 50 |
| Oriented grooves & scratches | | | | | 5 | 35 | 45 | 30 |
| Random grooves & scratches | 40 | 45 | 30 | 35 | 30 | 5 | 10 | |
| Pitted surface/collision pits | 20 | 25 | 35 | 30 | 20 | 5 | 5 | |
| Featureless smooth surfaces | 30 | 25 | 20 | 15 | 5 | 5 | | |
| <i>Chemical Textures</i> | | | | | | | | |
| Silica precipitation | 25 | 25 | 25 | 10 | 10 | | | |
| Adhering particles | 40 | 45 | 50 | 45 | 10 | 5 | | |
| Etched surfaces | 5 | 10 | 5 | 5 | | | | |
| Solution channels | 5 | | | | | | | |

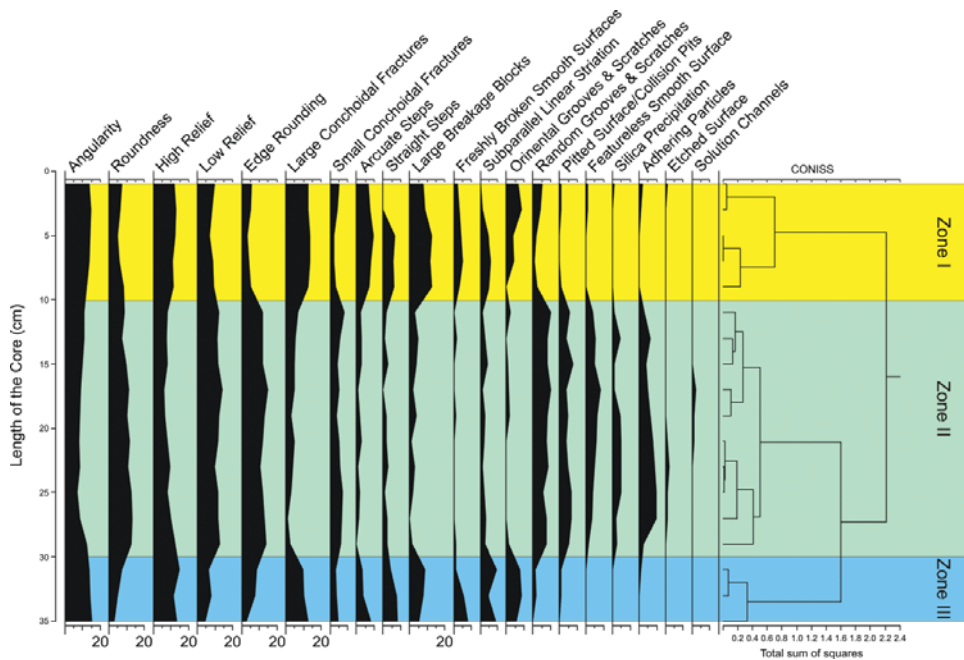


Fig. 4. CONISS Cluster Analysis on the percentage of the characteristics of grain morphology and microtextures (data in Table 2).

within the top 10 cm of the core. Zone II constitutes the next 10 samples within 10–30 cm of the core length. The last zone, Zone III, consists of only 3 samples of the bottommost part (30–36 cm) of the core. On the other hand, the core stratigraphy and sand percentage (Fig. 5) curve also shows some interesting results. Sand percentage of the core varies from 59.77% (32–34 cm) to 82.21% (6–8 cm). The 0–6 cm interval mostly shows sand with some granules and pebbles, which changes to an increase in granules downward up to 18 cm. The next 2 cm shows only sand, devoid of any granules and pebbles. The 20–32 cm interval exhibits silty sand which changes to sand with granules in the last 4 cm interval. Lithologically, the core exhibits fining downward up to 32 cm, followed by a coarsening downward trend. The top part (0–14 cm) shows sand percentage of more than 70%, while between 14–34 cm, sand percentage decreases below 70%. The last interval (34–36 cm) shows an increasing trend of sand percentage (Fig. 5).

AMS dates from the three lithological intervals are obtained as 3320 ± 35 yrs BP at 0 cm, 6145 ± 55 yrs BP at 14 cm and 12320 ± 50 yrs BP at 30 cm. These dates have been interpolated to get the age at each interval of the core, assuming a constant rate of sedimentation (Fig. 5). The extrapolated age at the bottommost sample of the core is 13.9 ka BP.

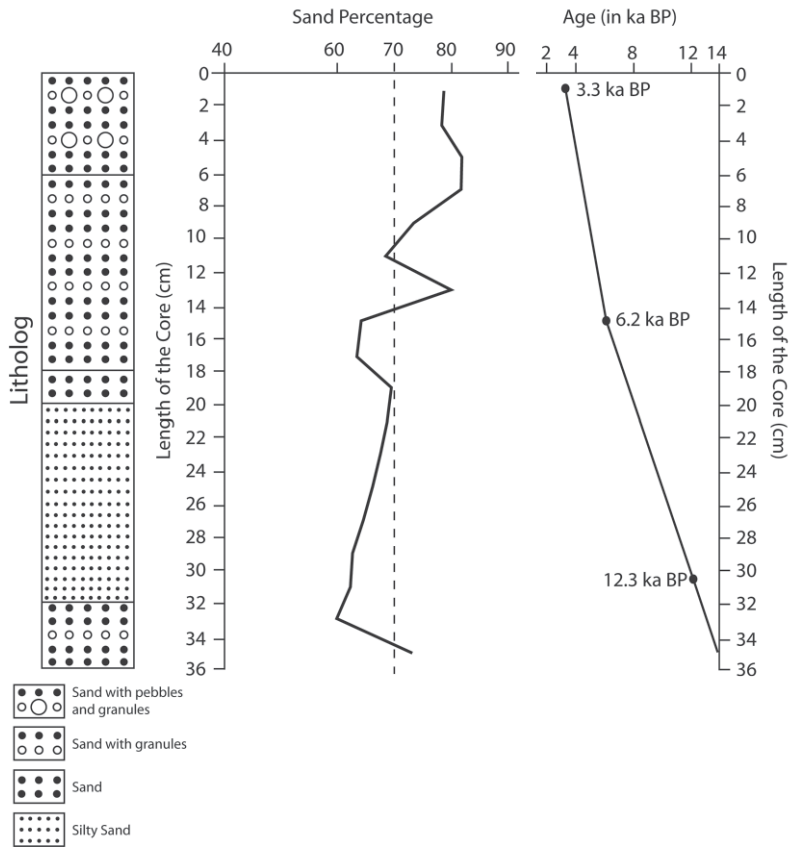


Fig. 5. Graph representing the core lithology, variation in sand percentage and the age along the core.

Discussion

Quartz microtextures as paleoenvironmental proxies. — The microtextures on the surface of detrital quartz grains are generally produced during transport and deposition of the sediments. SEM studies of the grain morphology and surface microtextures reflect the depositional environment and transport mechanism of the sediments (Krinsley and Donahue 1968; Margolis and Kennett 1971; Krinsley and Doornkamp 1973; Margolis and Krinsley 1974; Bull and Goudie 1987; Krinsley and Marshall 1987; Mazzullo 1987; Thomas 1987; Zhou *et al.* 1994; Mahaney 1995; Mahaney *et al.* 1996, 2001; Vos *et al.* 2014). In the polar environment, grain morphology and surface microtextures are commonly used to reconstruct the paleodepositional and paleoenvironmental history. Quartz grains mostly exhibit microtextures formed by high energy mechanical abrasion, which are characteristic features of glacial and eolian environments. The chemical

textures indicate the presence of the glacial melt water within the channels (Asthana and Chaturvedi 1998). The nature of the chemical textures varies due to the change in pH of the melt water while interacting with the sediments (Asthana and Chaturvedi 1998).

The quartz grains studied here mainly exhibit the textures of mechanical origin along with few occurrences of chemical origin. The grains show characteristic mechanical textures, such as angular grains, sub-angular grains, sub-rounded grains, rounded grains, arcuate fracture patterns, breakage blocks, oriented scratches and grooves, random scratches and grooves, large conchoidal fractures, small conchoidal fractures, parallel to sub-parallel steps, parallel to sub-parallel striations, collision pits, featureless smooth surfaces, and freshly broken smooth surfaces. Their environmental significance is summarised in Table 3. The textures of chemical origin, *viz.* adhering particles, secondary precipitation, solution channels and etched surfaces are also occasionally present. Depending on the morphology and texture characters, the mode of transportation and deposition can be classified mainly as glacial action with some aeolian and/or aqueous signatures at places (Krinsley and Doornkamp 1973; Asthana and Chaturvedi 1998) (Table 1). Angular to sub-angular grains along with arcuate fracture patterns, breakage blocks, oriented scratches and grooves, large conchoidal fractures, sub-parallel to parallel striations, sub-parallel to parallel steps and freshly broken smooth surfaces are indicative of glacial environment. On the other hand, rounded to sub-rounded grains along with rounded edges, collision pits, featureless smooth surfaces, small conchoidal fractures and random scratches and grooves reflect eolian environment. Aqueous environments are represented by the presence of adhering particles (along with glacial effect), silica precipitation, solution channels and etched surfaces.

Core zonation and paleoenvironments. — Depending on the percentages of the different sets of microtextures, CONISS Cluster Analysis was performed (Table 2 and Fig. 4). On the basis of zonation in Cluster Analysis, the entire core can be divided into three parts. Zone I, the upper part (0–10 cm), exhibits quartz grains with predominating characters of glacial activities, while Zone II, the middle part (10–30 cm), shows quartz grains with the characters of mostly glacial activities along with some prominent eolian and aqueous evidences, such as the presence of rounded to sub-rounded grains, random scratches and grooves (eolian environment) along with adhering particles, silica precipitation and solution channels (aqueous environment). Zone III, the lowest part (30–36 cm), predominantly shows a repeat of glacial activities. The top 0 to 14 cm shows higher (>70%) sand percentage (Fig. 5), which can be deciphered as an influence of glacial environment (Spaulding *et al.* 1997). The lithology of the core also shows sand along with pebbles and granules from 0 to 6 cm, followed by sand with granules up to 18 cm (Fig. 5). This also suggests that glacial activities

Table 3

Significance of the quartz grain microtextures along the core length for environmental assessment.

| Quartz grain surface textures | Environmental significance |
|-------------------------------------|----------------------------|
| Angular to sub-angular grains | Glacial |
| Arcuate fracture patterns | Glacial |
| Breakage blocks | Glacial |
| Oriented scratches and grooves | Glacial |
| Large conchoidal fractures | Glacial |
| Sub-parallel to parallel striations | Glacial |
| Sub-parallel to parallel steps | Glacial |
| Freshly broken smooth surfaces | Glacial |
| Adhering particles | Glacial + Aqueous |
| Silica precipitation | Aqueous |
| Solution channels | Aqueous |
| Etched surfaces | Aqueous |
| Rounded to sub-rounded grains | Eolian |
| Rounded edges | Eolian |
| Collision pits | Eolian |
| Featureless smooth surfaces | Eolian |
| Small conchoidal fractures | Eolian |
| Random scratches and grooves | Eolian |

increased upwards as supported by the coarsening of the grains towards the top. The next part (14 to 34 cm) exhibits lesser influence of glacial activities with an increase of eolian and aqueous depositional characters based on the lesser percentage (<70%) of sand which indicates an interglacial phase, where eolian and aqueous activities are more dominant, resulting in deposition of the finer particles. The lithology also exhibits sand from 18 to 20 cm, followed by silty sand up to 32 cm (Fig. 5). The presence of relatively finer particles indicates that the deposition was driven by comparatively lesser glacial influence. The lead-lag relation of ~800 yrs in mid to late Holocene and ~1500 yrs in early Holocene between quartz grain morphology and microtextures (represented by cluster zones) and the sand percentage is probably because of the gap between the processes of transportation and deposition. Quartz grain morphology and microtextures depend on the transportation, by transporting agents, while grain size variation in a basin occurs during the deposition. Hence, it is not always that the depositional characteristics chronologically match with the transportation

features due to the change over gap between these two processes; and the same has been observed in our present study area. The lowest part of the succession shows an increase in sand (>70%) along with the presence of granules (Fig. 5), which indicates the recurrence of glacial dominated environment in the study area.

Age model. — Chronology of the core represents sediment deposition between 13.9 ka and 3.3 ka. The interpolated ages at 10 cm and 30 cm exhibit 5.3 ka BP and 12.3 ka BP, respectively. On correlating the three cluster zones with the dates of the core, it is observed that from 5.3 ka BP to 3.3 ka BP (Cluster Zone I) glacial events predominated in the study area, which is repetitive of the previous glacial event prior to 12.3 ka BP (Cluster Zone III). Both these events are represented by extensive glacial microtextural and morphological signatures. On the other hand, 5.3 ka BP to 12.3 ka BP (Cluster Zone II) can be distinguished as a comparatively warmer period in this region, during which quartz grains with aqueous and eolian microtextural and morphological characteristics, are also present along with glacial derived sediments.

Regional context of paleoclimatic variability. — The onset of the Holocene (~11.5 ka BP) in Schirmacher Oasis was marked by a warming event, when the glaciers retreated from the low lying valleys leaving five major lakes in this region (Phartiyal *et al.* 2011). A previous study has also revealed that the Schirmacher Oasis was probably deglaciated at the Pleistocene–Holocene boundary (Gingele *et al.* 1997). This phenomenon is almost similar to that in the Larsemann Hills where the lakes were ice-free during 11.5 and 9.5 ka BP (Verleyen *et al.* 2003, 2004a, 2004b; Hodgson *et al.* 2004). This rise in temperature can be correlated with the commencement of the Holocene warming in other East Antarctic oases (Ingólfsson *et al.* 1998; Gore *et al.* 2001; Hodgson *et al.* 2001; Kirkup *et al.* 2002). In and around our study area, we also demarcated the glacial-interglacial boundary at 12.3 ka BP. Depending upon the data of magnetic susceptibility and loss-on-ignition from seven vertical sediment profiles, Phartiyal *et al.* (2011) hypothesized that the five major lakes in the Schirmacher Oasis existed until ~3 ka BP with intermittent climatic oscillations, which indicates the existence of a comparatively warmer climate until 3 ka BP. The major ice sheet recession in the East Antarctic region happened between ~12 and ~6 ka BP (Mackintosh *et al.* 2014). Our study also indicates a warmer climate in the area from 12.3 ka BP to 5.3 ka BP.

After this warm event, from 5.3 ka BP till 3.3 ka BP, our results show a colder period of glaciation. However, other studies have reported that the Schirmacher Oasis experienced warmer climatic conditions from 4.2 to ~2 ka BP as evident from the magnetic mineral concentrations and magnetic grain size parameters (Warrier *et al.* 2014). Phartiyal (2014) marked Phase 5 as a comparatively overall arid and cold period from 8.7 to 4.4 ka. However, Wagner *et al.* (2004) reported a short cooling

event from 6.7 to 3.7 ka BP in Amery Oasis just after the major early Holocene warm period. In Vestfold Hills region, a periodic warming and cooling alternation has been observed during 8.5–5.5 ka BP and 5.5–5.0 ka BP, respectively (Gibson unpublished results in Verleyen *et al.* 2011). The cluster analysis result (Fig. 5) shows two sub-zones under Zone I at 2.0 level of total sum of squares based on the percentage of different characteristics of grain morphology and microtextures. These two sub-zones indicate some differences of environment within Zone I. Chronologically, the lower subzone ranges from 5.3 ka BP to 4.1 ka BP, while the upper subzone ranges from 4.1 ka BP to 3.3 ka BP. The lower subzone definitely shows the signatures of intense glaciations by its grain morphology and microtextures, and this result is quite compatible with the short time glaciation periods in different parts of Antarctica, *viz.* Amery Oasis and Vestfold Hills. On the other hand, the upper subzones show less intensity of glacial evidences, which may indicate that the environment was again changing towards a warmer period after 4.1 ka BP. Thus, this time period can be assigned as a transitional period, when climate was changing from a colder to warmer period. The presence of late Holocene transitional period can be further looked into by more studies from the other lakes in the area.

Conclusion

In the present study, the higher sand percentage (>70%), along with the signatures of glacial nature depicted on quartz grains of the lake sediments, from a proglacial lake in the Schirmacher Oasis, records the predominantly colder conditions at the advent of Holocene. With the commencement of Holocene, glaciers started melting in this region, which is well manifested in the quartz grain microtextures. Mid-Holocene in this study is represented by the quartz grains having a characteristic mixture of glacial along with eolian and aqueous signatures, which is associated with lesser sand percentage value (<70%). This suggests the presence of relatively warmer climatic conditions in this region during that time. Late Holocene is represented by higher sand percentage (>70%) along with predominantly glacial marks in grain morphology and microtextures, which suggests the return of a glacial environment in this region. Thus, our study demarcates an early- to mid-Holocene warm period, sandwiched between two colder episodes during pre- and late-Holocene. Our data is well compatible with other studies on climatic history of Holocene in Antarctica, especially those from Amery Oasis and Vestfold Hills.

Acknowledgments. — The authors are grateful to the Director, Birbal Sahni Institute of Palaeosciences for providing permission to publish this paper. The authors thank the National Centre for Antarctic and Ocean Research, Goa, India for providing logistics and financial support. The authors thank Dr. Asit Kumar Swain, Geological Survey of

India, Faridabad and other members of 24th Indian Scientific Antarctic Expedition for their help to retrieve the sediment core from the lake and Dr. Rasik Ravindra, Ministry of Earth Sciences, New Delhi for his selfless help for quartz grain analysis. The authors are also thankful to Dr. Biswajeet Thakur for his help with CONISS Cluster Analysis and Tilia Software Program. The authors thank Dr. Kari N. Bassett and an anonymous reviewer for their useful suggestions.

References

- ASTHANA R. and CHATURVEDI A. 1998. The grain-size behaviour and morphoscopy of supraglacial sediments, south of Schirmacher Oasis, E. Antarctica. *Journal of Geological Society of India* 52: 557–568.
- BERA S.K. 2004. Late Holocene Palaeo-winds and climatic changes in Eastern Antarctica as indicated by long distance transported pollen-spores and local microbiota in polar lake core sediments. *Current Science* 86: 1485–1488.
- BULL P.A. and GOUDIE A.S. 1987. An examination of ability of environmental reconstruction by SEM studies: a case study from the plateau drift deposits of Oxfordshire, England. In: J.R. Marshall (ed.) *Clastic Particle: Scanning Electron Microscopy and Shape Analysis of Sedimentary and Volcanic Clasts*. Van Nostrand-Reinhold, New York: 36–50.
- CHAMLEY H. 1989. *Clay Sedimentology*. Springer, Berlin: 623 pp.
- GINGELE F., KUHN G., MAUS B., MELLES M. and SCHONE T. 1997. Holocene retreat from the Lazarev Sea shelf, East Antarctica. *Continental Shelf Research* 17: 137–163.
- GORE D.B., RHODES E.J., AUGUSTINUS P.C., LEISHMAN M.R., COLHOUN E.A. and REES-JONES J. 2001. Bunger hills, east Antarctica: ice free at the last glacial maximum. *Geology* 29: 1103–1106.
- GRIMM E.C. 2011. Tilia Software v.1.7.16. Springfield IL, Illinois State Museum 2011.
- HART J.K. 2006. An investigation of subglacial processes at the microscale from Briksdalsbreen, Norway. *Sedimentology* 53: 125–146.
- HELLAND P.E. and HOLMES M.A. 1997. Surface textural analysis of quartz sand grains from ODP Site 918 off the southeast coast of Greenland suggests glaciations of southern Greenland at 11 Ma. *Palaeogeography, Palaeoclimatology, Palaeoecology* 135: 109–121.
- HENDERSON P. and LAST W.M. 1998. Holocene sedimentation in Lake Winnipeg, Manitoba, Canada. *Journal of Paleolimnology* 19: 265–284.
- HODGSON D.A., DORAN P.T., ROBERTS D. and MCMINN A. 2004. Paleolimnological studies from the Antarctic and subantarctic islands. In: R. Pienitz, M.S.V. Douglas and J.P. Smol (eds) *Long-term Environmental Change in Arctic and Antarctic Lakes, Developments in Palaeoenvironmental Research*. Springer, Dordrecht: 419–474.
- HODGSON D.A., NOON P.E., VYVERMAN W., BRYANT C.L., GORE D.B., APPLEBY P., GILMOUR M., VERLEYEN E., SABBE K., JONES V.J., ELLIS-EVANS J.C. and WOOD P.B. 2001. Were the Larsemann hills ice-free through the last glacial maximum? *Antarctic Science* 13: 440–454.
- INGÓLFSSON Ó., HJORT C., BERKMAN P.A., BJÖRCK S., COLHOUN E.A., GOODWIN I.D., HALL B.L., HIRAKAWA K., MELLES M., MÖLLER P. and PRENTICE M.L. 1998. Antarctic glacial history since the Last Glacial Maximum: an overview of the record on land. *Antarctic Science* 10: 326–344.
- KIRKUP H., MELLES M. and GORE D.B. 2002. Late Quaternary environment of southern Windmill islands, east Antarctica. *Antarctic Science* 14: 385–394.
- KRINSLEY D.H. and DOORNKAMP J.C. 1973. *Atlas of quartz sand surface textures*. Cambridge University Press, Cambridge: 101 pp.

- KRINSLEY D.H. and DONAHUE J. 1968. Environmental interpretation of sand grain surface textures by electron microscopy. *Geological Society of American Bulletin* 79: 743–748.
- KRINSLEY D.H. and MARSHALL J.R. 1987. Sand grain textural analysis: an assessment. In: J.R. Marshall (ed.) *Clastic Particle: Scanning Electron Microscopy and Shape Analysis of Sedimentary and Volcanic Clasts*. Van Nostrand-Reinhold, New York: 2–15.
- KRUMBEIN W.C. and PETTJOHN F.J. 1938. *Manuel of sedimentary petrography*. Plenum, New York: 549 pp.
- LAST W.M. 2001. Mineralogical analysis of lake sediments. In: W.M. Last and J.P. Smol (eds) *Tracking Environmental Change Using Lake Sediments, Physical and Geochemical Methods, vol. 2*. Kluwer Academic Publishers, Dordrecht: 143–187.
- MACKINTOSH A.N., VERLEYEN E., O'BRIEN P.E., WHITE D.A., JONES R.S., MCKAY R., DUNBAR R., GORE D.B., FINK D., POST A.L., MIURA H., LEVENTER A., GOODWIN I., HODGSON D.A., LILLY K., CROSTA X., GOLLEDGE N.R., WAGNER B., BERG S., VAN OMMEN T., ZWARTZ D., ROBERTS S.J., VYVERMAN W. and MASSE G. 2014. Retreat history of the East Antarctic Ice Sheet since the Last Glacial Maximum. *Quaternary Science Review* 100: 10–30.
- MAHANEY W.C. 1995. Pleistocene and Holocene glacier thickness, transport histories and dynamics inferred from SEM microtextures on quartz particles. *Boreas* 24: 293–304.
- MAHANEY W.C. 2002. *Atlas of Sand Grain Surface Textures and Applications*. Oxford University Press, New York: 237 pp.
- MAHANEY W.C., CAMPBELL I.A. and CLARIDGE G. 1996. Microtextures on quartz grains in tills from Antarctica. *Palaeogeography Palaeoclimatology Palaeoecology* 121: 89–103.
- MAHANEY W.C., STEWART A. and KALM V. 2001. Quantification of SEM microtextures useful in sedimentary environmental discrimination. *Boreas* 30: 165–171.
- MAHESH B.S., WARRIER A.K., MOHAN R., TIWARI M., BABU A., CHANDRAN A., ASTHANA R. and RAVINDRA R. 2015. Response of Long Lake sediments to Antarctic climate: A perspective gained from sedimentary organic geochemistry and particle size analysis. *Polar Science* 9: 359–367.
- MARGOLIS S. and KRINSLEY D.H. 1974. Process of formation and environmental occurrence of microfeatures on detrital quartz grains. *American Journal of Science* 274: 449–464.
- MARGOLIS S.V. and KENNETT J.P. 1971. Cenozoic palaeoglacial history of Antarctica recorded in subantarctic deep sea cores. *American Journal Science* 271: 1–36.
- MATHUR A.K., MISHRA V.P. and SINGH J. 2009. Study of quartz grain surface texture by electron microscopy—a tool in evaluating palaeoglacial sediments in Uttarakhand. *Current Science* 96: 1377–1382.
- MAZZULLO J. 1987. Origin of grain shape types in the St. Peter Sandstone: determination by Fourier shape analysis and scanning electron microscopy. In: J.R. Marshall (ed.) *Clastic Particle: Scanning Electron Microscopy and Shape Analysis of Sedimentary and Volcanic Clasts*. Van Nostrand-Reinhold, New York: 302–313.
- MENKING K.M. 1997. Climatic signals in clay mineralogy and grain-size variations in Owens Lake core OL-92, southeast California. In: G.I. Smith and J.L. Bischoff (eds) *An 800,000-Year Paleoclimatic Record from Core OL-92, Owens Lake, Southeast California*. Geological Society of America, *Special Paper* 317: 37–48.
- OLSEN P.E. 1990. Tectonic, climatic, and biotic modulation of lacustrine ecosystems — examples from Newark supergroup of Eastern North America. In: B.J. Katz (ed.) *Lacustrine Basin Exploration, Case Studies and Modern Analogs*. AAPG Memoir 50: 209–224.
- PHARTIYAL B. 2014. Holocene paleoclimatic variation in the Schirmacher Oasis, East Antarctica: A mineral magnetic approach. *Polar Science* 8: 357–369.

- PHARTIYAL B., SHARMA A. and BERA S.K. 2011. Glacial lakes and geomorphological evolution of Schirmacher Oasis, East Antarctica, during Late Quaternary. *Quaternary International* 235: 128–136.
- PISTOLATO M., QUAlIA T., MARINONI L., VITTURI L.M., SALVI C., SALVI G., SETTI M. and BRAMBATI A. 2006. Grain size, mineralogy and geochemistry in late quaternary sediments from the western Ross sea outer slope as proxies for climate change. In: D.K. Fütterer, D. Damaske, G. Kleinschmidt, H. Miller and F. Tessensohn (eds) *Antarctica: Contributions to Global Earth Sciences*. Springer-Verlag, Berlin, Heidelberg, New York: 423–432.
- SCHÜTT B. 1998. Reconstruction of Holocene paleoenvironments in the endorheic basin of Laguna de Gallocanta, central Spain by investigation of mineralogical and geochemical characters from lacustrine sediments. *Journal of Paleolimnology* 20: 217–234.
- SHARMA C., CHAUHAN M.S. and SINHA R. 2007. Studies on Holocene climatic changes from Priyadarshini Lake sediments, East Antarctica: the palynological evidence. *Journal of Geological Society of India* 69: 92–96.
- SPAUDING S.A., MCKNIGHT D.M., STOERMER E.F. and DORAN P.T. 1997. Diatoms in sediments of perennially ice-covered Lake Hoare, and implications for interpreting lake history in the McMurdo Dry Valleys of Antarctica. *Journal of Paleolimnology* 17: 403–420.
- STANLEY S. and DEDECKER P. 2002. A Holocene record of allochthonous, aeolian mineral grains in an Australian alpine lake; implications for the history of climate change in southeastern Australia. *Journal of Paleolimnology* 27: 207–219.
- STRAND K., PASSCHIER S. and NASI J. 2003. Implications of quartz grain microtextures for onset Eocene/Oligocene glaciation in Prydz Bay, ODP site 1166, Antarctica. *Palaeogeography Palaeoclimatology Palaeoecology* 198: 101–111.
- THOMAS D.S.G. 1987. Discrimination of depositional environments using sedimentary characteristics in the mega Kalahari, central southern Africa. In: L.E. Frostick and I. Reid (eds) *Desert Sediments: Ancient and Modern*. Blackwell, London: 293–306.
- VERLEYEN E., HODGSON D.A., VYVERMAN W., ROBERTS D., MCMINN A., VANHOUTTE K. and SABBE K. 2003. Modelling diatom responses to climate induced fluctuations in the moisture balance in continental Antarctic lakes. *Journal of Paleolimnology* 30: 195–215.
- VERLEYEN E., HODGSON D.A., SABBE K., VANHOUTTE K. and VYVERMAN W. 2004a. Coastal oceanographic conditions in the Prydz Bay region (East Antarctica) during the Holocene recorded in an isolation basin. *The Holocene* 14: 246–257.
- VERLEYEN E., HODGSON D.A., SABBE K. and VYVERMAN W. 2004b. Late Quaternary deglaciation and climate history of the Larsemann hills (East Antarctica). *Journal of Quaternary Science* 19: 361–375.
- VERLEYEN E., HODGSON D.A., SABBE K., CREMER H., EMSLIE S.D., GIBSON J., HALL B., IMURA S., KUDOH S., MARSHALL G.J., MCMINN A., MELLES M., NEWMAN L., ROBERTS D., ROBERTS S.J., SINGH S.M., STERKEN M., TAVERNIER I., VERKULICH S., VAN DE VYVER E., NIEUWENHUYZE W.V., WAGNER B. and VYVERMAN W. 2011. Post-glacial regional climate variability along the East Antarctic coastal margin—Evidence from shallow marine coastal terrestrial records. *Earth-Science Reviews* 104: 199–212.
- VOS K., VANDENBERGHE N. and ELSSEN J. 2014. Surface textural analysis of quartz grains by scanning electron microscopy (SEM): From sample preparation to environmental interpretation. *Earth-Science Reviews* 128: 93–104.
- WAGNER B., CREMER H., HULTZSCH N., GORE D.B. and MELLES M. 2004. Late Pleistocene and Holocene history of Lake Terrasovoje, Amery Oasis, East Antarctica, and its climatic and environmental implications. *Journal of Paleolimnology* 32: 321–339.

- WARRIER A.K., MAHESH B.S., MOHAN R., SHANKAR R., ASTHANA R. and RAVINDRA R. 2014. Glacial–interglacial climatic variations at the Schirmacher Oasis, East Antarctica: The first report from environmental magnetism. *Palaeogeography Palaeoclimatology Palaeoecology* 412: 249–260.
- WARRIER A.K., PEDNEKAR H., MAHESH B.S., MOHAN R. and GAZI S. 2016. Sediment grain size and surface textural observations of quartz grains in late quaternary lacustrine sediments from Schirmacher Oasis, East Antarctica: Paleoenvironmental significance. *Polar Science* 10: 89–100.
- WHALLEY W.B. and KRINSLEY D.H. 1974. A scanning electron microscope study of surface textures of quartz grains from glacial environments. *Sedimentology* 21: 87–105.
- ZHOU L., WILLIAMS M.A.J. and PETERSON J.A. 1994. Late Quaternary aeolianites, palaeosols and depositional environments on the Nepean Peninsula, Victoria, Australia. *Quaternary Science Review* 13: 225–239.

Received 16 June 2016

Accepted 16 January 2017